Electronic structure of $SrVO_3$(001) surfaces: A local-density approximation plus dynamical mean-field theory calculation

H. Ishida,[1] D. Wortmann,[2] and A. Liebsch[2]
[1]*CREST JST and College of Humanities and Sciences, Nihon University, Tokyo 156-8550, Japan*
[2]*Institut für Festkörperforschung, Forschungszentrum Jülich, 52425 Jülich, Germany*
(Received 12 April 2006; published 19 June 2006)

The influence of local Coulomb correlations on the surface electronic structure of $SrVO_3$, a strongly-correlated metal in a perovskite structure, is investigated for both the SrO-layer and VO_2-layer-terminated (001) surfaces. The electronic structure within the local density approximation of a semi-infinite surface is determined using the embedded Green-function approach, and the resultant density of states projected on the V t_{2g} orbitals is used as an input to a subsequent many-body calculation within the dynamical mean field theory (DMFT) and the multiorbital quantum Monte Carlo technique. Qualitatively, the present study confirms the conclusion of recent photoemission experiments and tight-binding DMFT calculations which both indicate that the electronic structure at the surface is more strongly correlated than in the bulk. On a quantitative level significant differences are obtained as a function of orbital polarization at the surface, surface layer relaxation, and SrO vs VO_2 surface termination.

DOI: 10.1103/PhysRevB.73.245421 PACS number(s): 73.20.At, 71.27.+a, 71.30.+h

I. INTRODUCTION

Transition-metal oxides have been extensively studied as typical strongly correlated materials. They exhibit phenomena such as metal-insulator transition and superconductivity, whose understanding is at the center of current solid state research.[1–3] The electronic structure of transition-metal oxides is essentially determined by the energy dispersion of transition-metal d bands, their occupancies, and the on-site Coulomb and exchange energies among the d orbitals.[4] Their properties can be greatly varied by applying pressure and by chemically substituting nontransition-metal cation species, which has enabled a systematic study of the phase diagram of these materials (known as bandwidth control and filling control).[1] As a result of this extreme sensitivity to key material parameters it is not surprising that the electronic structure of transition-metal oxides may change at the surface due to the reduced coordination of surface atoms, lower symmetry, surface reconstruction, and less efficient surface screening processes.

Recently, surface effects in photoemission from transition-metal oxides were reported by several groups.[5–11] Maiti *et al.* proposed an algorithm for extracting bulk and surface contributions to total photoemission spectra by exploiting the dependence of photoelectron escape length on the incident photon energy.[5] Their study for $Ca_xLa_{1-x}VO_3$ ($0 \leq x \leq 0.5$) suggested that bulk electronic properties become metallic at $x \geq 0.2$, while the surface might remain insulating in the entire x range.[5,8] Maiti *et al.* and Sekiyama *et al.* performed photoemission measurements on $Ca_xSr_{1-x}VO_3$ for a wide range of photon energies.[9,10] They found that at the surface the spectral weight of the coherent peak at the Fermi energy (E_F) is reduced, while that of the incoherent satellite peak is enhanced. These experiments indicated that the electronic structure at the surface is more correlated than in the bulk.

Stimulated by these experimental observations, one of the present authors (A.L.) initiated a theoretical investigation of the electronic structure of perovskite-type transition-metal oxides at the surface.[12,13] A semi-infinite cubic tight-binding Hamiltonian was employed to represent the t_{2g} bands and the layer-resolved density of states (DOS) was then used as an input to many-body Green-function calculations within the dynamical mean field theory [2,14,15] (DMFT), combined with the quantum Monte Carlo[16,17] (QMC) method. The perovskite t_{2g} bands consist of two subbands (xz, yz) which hybridize predominantly in a plane perpendicular to the surface and of a third one (xy) which hybridizes mainly within the surface plane. It was shown that the reduced coordination number of surface atoms leads to an effective narrowing of the xz, yz bands. Nevertheless, as a result of intra- and interorbital Coulomb interactions the surface quasiparticle spectra of all three t_{2g} bands exhibit stronger correlation features than in the bulk, in qualitative agreement with the above-mentioned experiments.

It is well known that, besides the reduced coordination number in the normal direction, several other effects, such as reconstruction and relaxation, may cause the single-particle electronic structure at the surface to differ considerably from that in the bulk. Unfortunately, it is not possible to self-consistently determine the one-electron parameters at the surface within a tight-binding approach. To evaluate the surface electronic properties from first principles we perform a calculation within the local density approximation[18] (LDA) and the full-potential linearized augmented plane-wave (FLAPW) approach, combined with the embedded Green-function technique.[19] In the present work the focus is on the (001) surface of $SrVO_3$ which has attracted much attention in recent years.[9–11] To our knowledge no experimental studies on the detailed atomic structure of the $SrVO_3$ surface have been carried out until now. Recent angle-resolved photoemission experiments found no evidence of a superstructure giving rise to band foldings.[11] Therefore, in the present work we consider unreconstructed surfaces, without any lateral rearrangement of atoms. Instead we focus on two effects: (i) surface relaxation, i.e., displacement of the outermost atomic

plane from its ideal bulk position, and (ii) surface termination, i.e., outermost planes consisting of a SrO or VO_2 layer. We calculate the electronic structure of each surface within the LDA and use the resultant local DOS projected on V t_{2g} orbitals as an input to a subsequent multiband QMC/DMFT calculation.

The main result of this work is that, although the quasiparticle spectra of all of the surface structures considered exhibit more pronounced correlation features compared to the bulk, the degree of enhancement depends sensitively on the details of the local density of states, in particular, the orbital polarization caused by charge transfer among t_{2g} bands. This is a genuine surface effect since in the bulk the cubic environment yields degenerate t_{2g} orbitals.

The plan of the paper is as follows: In Sec. II we briefly explain the embedded Green-function method and the DMFT approach. Section III presents the results and discussion of the single-electron features of the surface electronic structure. Section IV contains the discussion of the correlation effects associated with the surface. A summary is given in Sec. V. We use the Hartree atomic units throughout the paper unless otherwise stated.

II. METHOD

The first step in the LDA+DMFT approach is the electronic-structure calculation within LDA. Since we intend to compare surface and bulk electronic properties of $SrVO_3$, it is crucial that the calculated local DOS of surface V atoms has the same accuracy as that of bulk atoms. Standard surface calculations within a slab approximation are not suitable for this purpose, as the calculated DOS exhibits spurious spiky peaks due to discretization of energy levels in the surface normal direction. In the present work we treat a truly semi-infinite surface of $SrVO_3$ by using the embedding technique of Inglesfield.[20,21] In this method one considers explicitly a surface region with finite thickness which contains the first few atomic layers. The effects of the semi-infinite substrate and the vacuum are incorporated via embedding potentials acting on boundary surfaces on both sides of the surface region. The embedding calculation proceeds in three steps: (i) calculating the bulk crystal potential of $SrVO_3$ using a bulk electronic-structure code, (ii) constructing the embedding potential for the (001) orientation from the corresponding complex band structure,[22,23] and (iii) performing a self-consistent electronic-structure calculation in the embedded surface region. We use a code that combines the embedded Green-function technique and the full-potential linearized augmented plane-wave (FLAPW) method.[19]

As stated in the Introduction, we consider the (001) surface terminated both with a SrO and a VO_2 layer. It is to be noted that both lattice planes possess no formal charges. For the former case we embed two SrO layers and two VO_2 layers in the embedded surface region as shown in Fig. 1(a). This amounts to ten atoms per surface unit cell. For the latter case, three outermost atomic layers are included in the embedded region as shown in Fig. 1(b). The lattice constant of bulk $SrVO_3$ is 7.26 a.u., the cut-off energy for the plane wave part of the LAPW basis functions is 14.4 Ry, and the

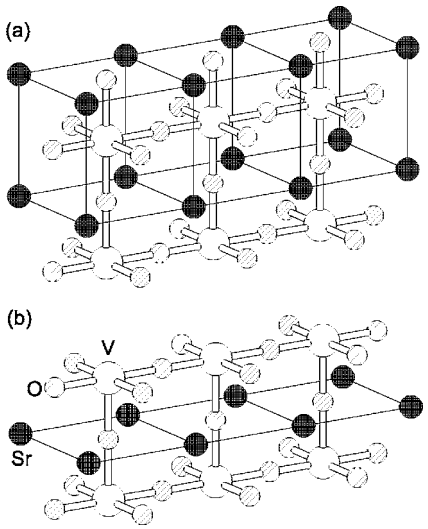

FIG. 1. Structure models of the $SrVO_3$(001) surface. (a) Surface terminated with a SrO lattice layer, and (b) surface terminated with a VO_2 layer. The z axis is chosen as the surface normal.

maximum angular momentum for partial wave expansion inside muffin-tin (MT) spheres for the LAPW basis is chosen as $l_{\max}=9$. In addition to ideal cleaved surfaces, we consider relaxations of top-layer atoms in the normal direction. Since the force calculation is not yet implemented in the embedded Green-function code, we utilize the slab version of the FLEUR code to optimize the atomic geometry.[24]

In the second step we treat the effect of local Coulomb correlations on quasiparticle spectra within the DMFT.[2,14,15] We adopt a simplified version of finite-temperature DMFT in which the local Green function of a surface V atom is approximated by

$$G_i(i\omega_n) = \int_{-\infty}^{+\infty} d\epsilon \frac{\rho_i(\epsilon)}{i\omega_n + \mu - \epsilon - \Sigma_i(i\omega_n)}, \qquad (1)$$

where ω_n is the Matsubara frequency, μ is the chemical potential, and i is the index for the t_{2g} orbitals, $\{d_{xy}, d_{xz}, d_{yz}\}$. The z axis is chosen as the surface normal pointing to the vacuum. In Refs. 12 and 13 $\rho_i(\epsilon)$, the local DOS projected on orbital i, was calculated using a semi-infinite cubic tight-binding model. In the present work we employ a more realistic DOS obtained from the first-principles calculation described above. In Eq. (1), $\Sigma_i(i\omega_n)$ is the onsite self-energy of orbital i which characterizes the effect of local Coulomb correlations. As we do not consider the relaxation of surface atoms within the plane which would lift the C_{4v} symmetry at a V site, the self-energy is diagonal with respect to orbital i. In contrast to the bulk where the self-energies for the three t_{2g} bands are the same, at the surface Σ_{xy} deviates from $\Sigma_{xz,yz}$.

In principle, Eq. (1) is valid only when the self-energy is site-independent. In the present case we confront a problem of treating a semi-infinite system with layer-dependent self-energies. Unfortunately, a full description of Coulomb correlations for such an inhomogeneous system is still exceedingly complicated. Here we consider only the primary effect

and assume that the reduced dimensionality at the surface enters the theory through the layer-dependent DOS, $\rho_i(\epsilon)$. In view of the local Coulomb interaction, this assumption should be justified for qualitative purposes. We refer to Refs. 12 and 13 for further discussions.

Starting from an input self-energy, within DMFT one calculates the bath Green-function $\mathcal{G}_i(i\omega_n)$ as $(\mathcal{G}_i)^{-1}=(G_i)^{-1}+\Sigma_i$, which gives a mean-field Hamiltonian at the V site under consideration. Then one adds to this effective one-electron Hamiltonian a correlation term,

$$\hat{\mathcal{H}}_I=\sum_i U\hat{n}_{i\uparrow}\hat{n}_{i\downarrow}+\sum_{\substack{i,j,\sigma,\sigma'\\(i\neq j)}}(U'-J\delta_{\sigma\sigma'})\hat{n}_{i\sigma}\hat{n}_{j\sigma'}, \qquad (2)$$

where U and $U'=U-2J$ are intraorbital and interorbital Coulomb matrix elements and J is the exchange interaction. As a result of less efficient screening these interaction energies are likely to be somewhat larger at the surface than in the bulk. Since there are so far no theoretical estimates of this effect, bulk values of U and J will be used in the calculations discussed below. The single-site impurity problem which is solved using the multiband quantum Monte Carlo technique yields a new many-body Green-function G_i. A new self-energy is then derived by using again the relation $\Sigma_i=(\mathcal{G}_i)^{-1}-(G_i)^{-1}$. This procedure is iterated until the difference between the input and output self-energies becomes sufficiently small.

III. LDA RESULTS

The calculated work function of the ideal $SrVO_3$ surface terminated with a SrO layer is only 1.3 eV, suggesting that the outermost SrO layer is slightly positively charged. This value increases to 2.6 eV when the atoms in the top SrO plane are relaxed to minimal-energy positions. As stated in Sec. II, the atomic geometry was optimized using the FLEUR code[24] and a slab model consisting of five VO_2 and six SrO layers. The calculated displacements in the z direction of the O and Sr atoms are +0.07 a.u. (outward) and −0.37 a.u. (inward), respectively. The rather small displacement of the top-layer O atoms signifies that the local octahedral symmetry of outermost V ions is only slightly disturbed. We performed an additional calculation where the V and O atoms in the second layer were also allowed to relax. The atomic displacements obtained are smaller than 0.02 a.u. and give rise to only insignificant changes in the electronic structure at the V site. For the VO_2-layer-terminated surface, the surface geometry was optimized using a slab consisting of four VO_2 layers and three SrO layers. The calculated displacements in the z direction of the top VO_2 layer, −0.13 a.u. for the V site and +0.05 a.u. for the O site, with respect to the ideal positions are rather small. The corresponding work functions for the ideal and relaxed surfaces are 4.4 eV and 4.8 eV, respectively.

The orbital-decomposed DOS of a V atom within LDA is calculated from the imaginary part of the Green function as

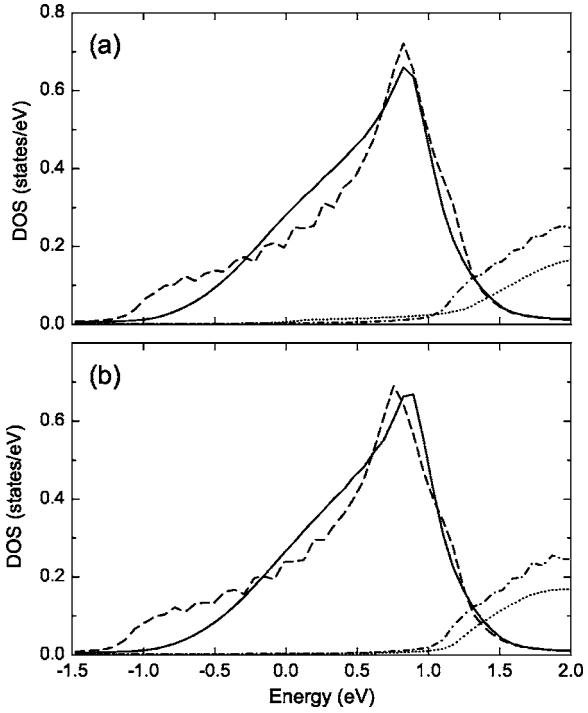

FIG. 2. The local DOS projected on 3d orbitals of an outermost V atom for (a) ideal and (b) relaxed $SrVO_3$ surfaces terminated with a SrO layer. R=2.05 a.u. and η=0.07 eV. Solid, dashed, dotted, and dashed-dotted lines correspond to the xz/yz, xy, $3z^2-r^2$, and x^2-y^2 components, respectively.

$$\rho_i(\epsilon)=\frac{-1}{\pi}\int\frac{d\mathbf{k}}{(2\pi)^2}\int_0^R r^2dr\langle i|\Im G(\mathbf{r},\mathbf{r},\epsilon+i\eta,\mathbf{k})|i\rangle, \qquad (3)$$

where $|i\rangle$ denotes the lattice harmonics corresponding to orbital i, and R is the MT radius of a V atom. At a given two-dimensional (2D) wave vector $\mathbf{k}$ in the surface Brillouin zone (SBZ), the DOS projected on orbital i is a smooth function of energy ϵ for the xz/yz orbitals, whereas the DOS for the xy orbital appears nearly as a discrete state because of the quasi-2D nature of the xy band. Since in numerical calculations the integral over $\mathbf{k}$ in Eq. (3) is replaced by a summation with an appropriate weight function we introduce a finite imaginary energy η so that $\rho_i(\epsilon)$ for the xy orbital becomes a smooth function of energy ϵ.

As is well known, the valence electronic structure of $SrVO_3$ is characterized by O 2p bands, located between −7 and −2 eV below E_F, and by V 3d bands, located between −1 and +5 eV relative to E_F.[25] Due to the octahedral symmetry, the V 3d bands split into the three t_{2g} bands at lower energies and the two e_g bands at higher energies. E_F crosses the t_{2g} bands, which accommodate one electron. In Fig. 2 we show the local DOS projected on five 3d orbitals of an outermost V atom for the $SrVO_3$ surfaces terminated with a SrO layer in the energy range corresponding to the V t_{2g} band. Here E_F is chosen as the origin of energy. Reflecting the relatively small distortion of the octahedron surrounding a V atom in the outermost VO_2 plane, the calculated DOS's for the ideal and relaxed surfaces are quite similar.

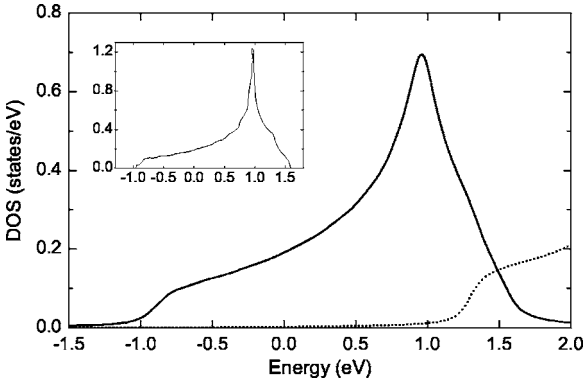

FIG. 3. The local DOS projected on t_{2g} (solid line) and e_g (dotted line) orbitals of a V atom in bulk $SrVO_3$ with $R=2.05$ a.u. The inset shows the t_{2g} DOS without broadening. The curves in the main panel are broadened using the Lorentz distribution of width $\eta=0.07$ eV.

For comparison, we show in Fig. 3 the corresponding local DOS of a V atom in bulk $SrVO_3$ obtained using a bulk FLAPW code. The t_{2g} DOS in the inset was calculated using a standard tetrahedron method for a three-dimensional bulk system, which is in good agreement with previous calculations.[25–27] It exhibits a characteristic asymmetric peak related to the Van Hove singularity according to the quasi-2D electronic structure. This DOS curve was further broadened using a Lorentz distribution with the same width parameter η as in Eq. (2) for the sake of a better comparison with the surface calculation. The resultant DOS's for the t_{2g} and e_g orbitals are shown in the main panel of Fig. 3.

It is seen that the overall shape of $\rho_{xy}(\epsilon)$ in Fig. 2 is very similar to that of the bulk t_{2g} DOS in Fig. 3 as may be expected from the quasi-2D character of the xy band. At a closer look one finds that its position is shifted toward lower energies as compared to that of the bulk t_{2g} band, which can be attributed to a change in the onsite energy at the V site. The shift amounts to 0.2 and 0.25 eV for the ideal and relaxed geometries, respectively. As a consequence, at a fixed **k** point, one observes two distinct peaks in the **k**-resolved d_{xy} DOS, a dominant one at a lower energy corresponding to the xy band of the surface layer and a small one at a higher energy originating from the wave-function tail of the bulk xy band. In contrast, the DOS for the xz/yz band at a fixed **k** point forms a broad spectrum owing to their energy dispersion with wave number in the z direction and exhibits no distinct surface states in the spectrum. Thus, when integrated over the SBZ, $\rho_{xz,yz}(\epsilon)$ in Fig. 2 appears in the same energy range as that of the bulk t_{2g} band. However, its shape is appreciably different from that of the bulk t_{2g} band; its weight is reduced at low and high energies but enhanced at intermediate energies. The same qualitative trend was found previously in the semi-infinite tight-binding calculation.[12,13] Thus, the effective width of $\rho_{xz,yz}(\epsilon)$ is smaller than that of the bulk t_{2g} DOS although their total widths are identical.

The above-mentioned change in position and shape of $\rho_i(\epsilon)$ results in increase or decrease in the occupation number of orbital i inside a V MT sphere, n_i, defined as $n_i = \int^{E_F} \rho_i(\epsilon) d\epsilon$. To avoid effects of the broadening parameter η, we use a semicircular contour ending at E_F in the complex energy plane in evaluating n_i. In Table I we compare n_i of the t_{2g} orbitals in the bulk with the corresponding ones of an outermost V atom at the surface. It should be noted that the sum of n_i in the bulk is smaller than unity because n_i is calculated in a MT sphere with a fixed radius $R=2.05$ a.u. For a SrO-layer-terminated surface, the effective reduction in width of $\rho_{xz,yz}(\epsilon)$ leads to the decrease in $n_{xz,yz}$, while the downward shift of $\rho_{xy}(\epsilon)$ leads to the increase in n_{xy}. This surface, therefore, is characterized by a sizable interorbital charge transfer from xz,yz to xy by about 13% or 29% for the ideal or relaxed geometries, respectively.

TABLE I. Occupations of t_{2g} orbitals calculated in a V muffin-tin sphere with radius $R=2.05$ a.u.

		SrO-terminated		VO_2-terminated	
	Bulk	Ideal	Relaxed	Ideal	Relaxed
$n_{xz,yz}$	0.24	0.21	0.19	0.31	0.28
n_{xy}	0.24	0.27	0.31	0.12	0.13
Total	0.72	0.69	0.69	0.74	0.69

In order to illustrate the convergence of the electronic properties with distance from the surface, we show in Fig. 4 the local DOS projected on V $3d$ orbitals in the second VO_2 plane. One notices an oscillatory distortion in the shape of $\rho_{xz,yz}(\epsilon)$, which originates from the interference of electronic states incident from the interior with the waves reflected at the surface. The same behavior was observed in the tight-binding calculation.[12,13,28] On the other hand, $\rho_{xy}(\epsilon)$ becomes nearly identical with the bulk t_{2g} DOS in Fig. 2 including not only its shape but also its position. Thus, the potential change due to the surface and the concomitant interorbital charge transfer decay very rapidly with distance from the surface.

Next, we consider the $SrVO_3(001)$ surface terminated with a VO_2 layer. One may expect a larger change in the electronic structure of the outermost V site since the loss of one apex O atom greatly disturbs the local octahedral symmetry. Figure 5 shows the calculated local DOS projected on

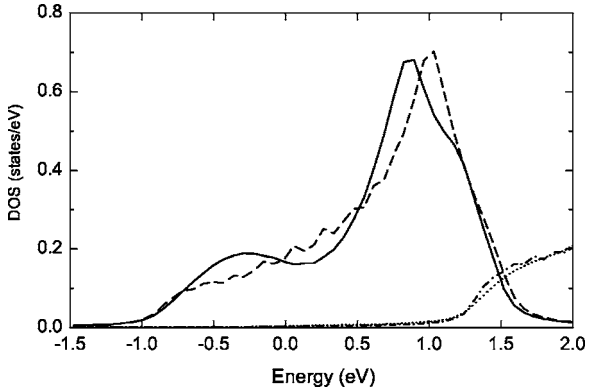

FIG. 4. The local DOS projected on $3d$ orbitals of a V atom in the second VO_2 plane for an ideal $SrVO_3$ surface terminated with a SrO layer. $R=2.05$ a.u. and $\eta=0.07$ eV. Solid, dashed, dotted, and dashed-dotted lines correspond to the xz/yz, xy, $3z^2-r^2$, and x^2-y^2 components, respectively.

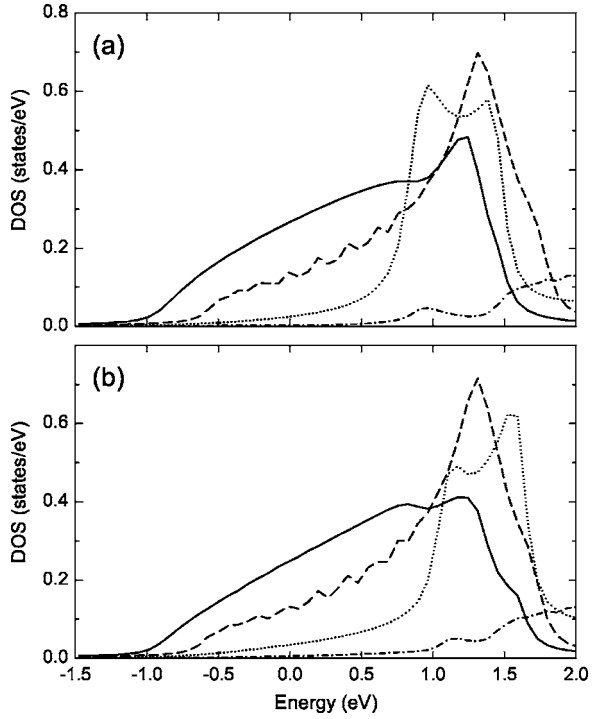

FIG. 5. The orbital-decomposed DOS of an outermost V atom for (a) ideal and (b) relaxed $SrVO_3$ surfaces terminated with a VO_2 layer. $R=2.05$ a.u. and $\eta=0.07$ eV. Solid, dashed, dotted, and dashed-dotted lines correspond to the xz/yz, xy, $3z^2-r^2$, and x^2-y^2 components, respectively.

$3d$ orbitals of an outermost V atom for the ideal and relaxed $SrVO_3$ surfaces terminated with a VO_2 layer. Compared to the bulk and SrO terminated surface several pronounced changes occur: (i) The $d_{3z^2-r^2}$ surface band is shifted far below the bulk e_g band and forms a relatively narrow spectrum at about 0.8–1.5 (1.0–1.7) eV above E_F. This implies that the $d_{3z^2-r^2}$ band in the top layer becomes a localized 2D surface band. [We note that the long tail of $\rho_{3z^2-r^2}(\epsilon)$ is an artifact of the Lorentz broadening; $n_{3z^2-r^2}$ is negligibly small.] (ii) The shape of the $d_{xz,yz}$ DOS is also greatly modified compared to the t_{2g} DOS in Fig. 3, but the band appears in the same energy range as that of the bulk band. Thus, no surface band is formed from the $d_{xz,yz}$ state. Nevertheless, the density of states below E_F is considerably enhanced, implying an interorbital charge transfer that is opposite to the one found for the SrO terminated surface. (iii) Owing to the quasi-2D character of the d_{xy} states, their local density of states is affected to a much lesser degree by the missing apical O atom. However, their position shifts by ~ 0.3 eV toward higher energies compared to the bulk, implying about 50% reduced orbital occupation. The details of this charge rearrangement among t_{2g} orbitals are given in Table I. As we discuss in the next section this surface induced redistribution of valence charge has significant consequences for the influence of Coulomb interactions on the t_{2g} quasiparticle spectra.

IV. DMFT RESULTS

In this section, we treat the effects of local Coulomb correlations on the excitation spectra of an outermost V atom within LDA+DMFT. For this purpose, we use the orbital-decomposed DOS shown in Figs. 2 and 5 as an input to Eq. (1). Since the DOS functions calculated in a MT sphere with a given radius are not normalized to unity, each of them is multiplied by a constant such that the resultant renormalized $\rho_i(\epsilon)$ accommodates exactly one electron per band when integrated over the whole energy range. This procedure should qualitatively account for the V $3d$ charge hybridizing with O $2p$ states.

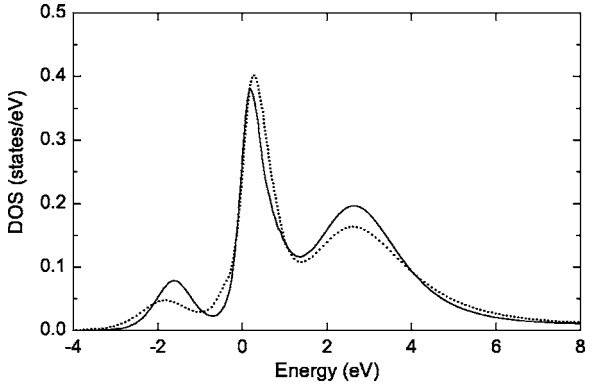

FIG. 6. Bulk quasiparticle spectra of a V atom in $SrVO_3$ derived from LDA+DMFT for $U=5.55$ eV and $J=1$ eV. Solid (dotted) curve: input from unbroadened (broadened) bulk DOS, as shown in Fig. 3.

Besides $\rho_i(\epsilon)$, the inputs to a DMFT calculation are the local Coulomb parameters, the filling of the t_{2g} bands, $n_{t_{2g}}$, and temperature $T=\beta^{-1}$. It is plausible that $n_{t_{2g}}$ at the surface deviates from the bulk configuration $(3d)^1$ due to charge redistributions between and within surface layers. As a qualitative estimate, we choose to use a ratio of the total t_{2g} occupation calculated in a V MT sphere in the bulk and that at the surface which are tabulated in the third row of Table I. For example, for the ideal or relaxed surfaces terminated with a SrO layer, $n_{t_{2g}}=0.69/0.72=0.96$ is used as an input to the DMFT calculation. The same value applies to the relaxed surface with VO_2 layer termination, while the unrelaxed case has $n_{t_{2g}}=0.74/0.72=1.03$. The effects of $n_{t_{2g}}$ on the quasiparticle spectra of V atoms are found to be rather modest as long as its variation from the bulk value $n_{t_{2g}}=1$ is less than 0.05. More important are the local Coulomb energies: In the present work, we adopt $U=5.55$, $J=1$, and $U'=U-2J=3.55$ eV, which were determined by Nekrasov *et al.* using the constrained LDA method for a bulk crystal.[26] As it is likely that the Coulomb energies are enhanced at the surface due to less efficient surface screening processes, the results discussed below should be regarded as representing a case where correlation effects are tuned to a minimum.

As a reference system, we show in Fig. 6 the bulk quasiparticle spectra of $SrVO_3$ for $\beta=8$ eV^{-1} ($T=1450$ K), which was derived from the imaginary-time Green function using the maximum entropy technique.[29] The solid line represents the quasiparticle DOS calculated using the tetrahedron t_{2g} DOS in the inset of Fig. 3. It exhibits a coherent peak straddling E_F, and the lower and upper Hubbard bands characteristic of a strongly correlated electron system. The line shape is in good agreement with a recent calculation of Nekrasov *et*

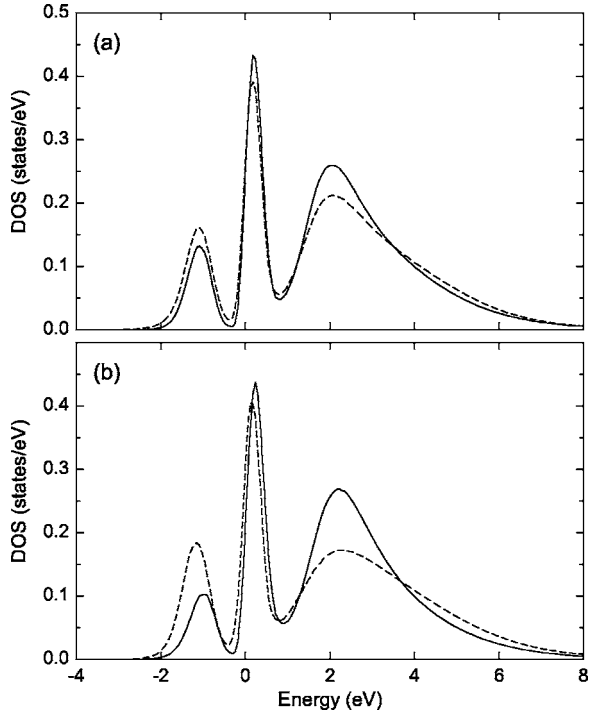

FIG. 7. Quasiparticle spectra of an outermost V atom for (a) ideal and (b) relaxed $SrVO_3$ surface terminated with a SrO layer. $U=5.55$ eV and $J=1$ eV. Solid and dashed lines correspond to the xz/yz and xy components, respectively.

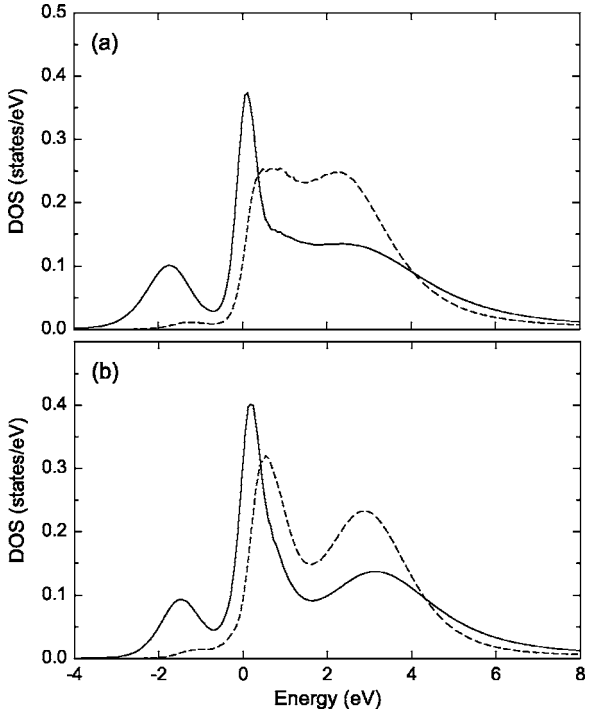

FIG. 8. Quasiparticle DOS of an outermost V atom for (a) ideal and (b) relaxed $SrVO_3$ surfaces terminated with a VO_2 layer. $U=5.55$ eV and $J=1$ eV. Solid and dashed lines correspond to the xz/yz and xy components, respectively.

al.[26,27] Since the LDA DOS in Figs. 2 and 5 includes a Lorentz broadening, it is necessary to check how this additional broadening affects the V quasiparticle spectra. The bulk DMFT calculation was therefore repeated for the LDA DOS in the main panel of Fig. 3, using the same broadening parameter $\eta=0.07$ eV. The result is shown by the dotted line in Fig. 6. As may be expected, the lower and upper Hubbard bands are less pronounced than for the unbroadened DOS. Nevertheless, the qualitative features of the spectral distribution, in particular, the peak positions, remain nearly intact for the present choice of η.

Figure 7 shows the calculated xz/yz and xy quasiparticle spectra of a V atom at the surface of $SrVO_3$ with SrO-layer termination. The comparison with the bulk spectra shown in Fig. 6 demonstrates that correlation effects for a fixed value of U are enhanced at the surface. The coherent peaks of both the $d_{xz/yz}$ and d_{xy} contributions are narrower at the surface and the incoherent satellite features are more pronounced than in the bulk, in qualitative agreement with recent experiments [9,10] and with previous tight-binding calculations.[12,13] It should be noted that correlation effects would be further reinforced if the spectra were calculated using the LDA DOS without broadening. According to Fig. 2, the $d_{xz/yz}$ surface DOS is effectively narrower than the d_{xy} DOS. One might therefore expect the $d_{xz/yz}$ quasiparticle spectrum to be more strongly correlated. However, the local Coulomb interaction mixes both bands, so that this difference will be reduced. More importantly, according to Table I, the d_{xy} surface band has a larger occupation than the $d_{xz/yz}$ band. As a result, the d_{xy} band turns out to be even more strongly correlated than the $d_{xz/yz}$ band. In fact, in order to be able to accommodate more electrons, the lower Hubbard peak of the d_{xy} DOS for the relaxed structure [Fig. 7(b)] is seen to be substantially larger than that of the $d_{xz/yz}$ band. In this case the filling ratio between the two bands, $n_{xy}/n_{xz,yz}$, is 1.75, which is even larger than the corresponding LDA value, 1.6. Thus, the surface-induced interorbital charge transfer from $d_{xz/yz}$ to d_{xy} states is further enhanced via local Coulomb correlations.

We now proceed to the discussion of the quasiparticle spectra of the VO_2-layer-terminated surfaces. As discussed in the preceding section, the long tail of $\rho_{3z^2-r^2}(\epsilon)$ on the low energy side in Fig. 5 is an artifact of the Lorentz broadening introduced in the LDA DOS. The lower edge of the $d_{3z^2-r^2}$ band at $\mathbf{k}=0$ is located at 0.8 and 1.0 eV above E_F for the ideal and relaxed surfaces, respectively. Thus, in the present work the multiband QMC calculation is carried out using the three t_{2g} states without incorporating the $d_{3z^2-r^2}$ orbital into it, as in the case of the SrO-layer-terminated surfaces. Figure 8 shows the calculated quasiparticle DOS of an outermost V atom for the ideal and relaxed $SrVO_3$ surfaces terminated with a VO_2 layer. According to Fig. 5, $\rho_{xz,yz}(\epsilon)$ has a much weaker van Hove singularity and its spectral weight is more evenly spread out over the band width than for the SrO layer terminated surface. Thus, in the quasiparticle spectra shown in Fig. 8 the satellite peaks (especially the upper Hubbard band) are less pronounced and the coherent peak is slightly broader than in the spectra shown in Fig. 7. A more dramatic effect occurs as a result of the surface-induced orbital polarization. According to Table I the $d_{xz,yz}$ band is more populated on this surface than the d_{xy} band. Local Coulomb correlations further promote this interorbital charge transfer from d_{xy} to $d_{xz,yz}$. The ratios $n_{xy}/n_{xz,yz}$ calculated via the

DMFT are now 0.19 and 0.25 for the ideal and relaxed surfaces, respectively, which are a factor 2 smaller than the corresponding LDA values (see Table I). Thus, the d_{xy} band becomes nearly depleted at the VO_2-terminated surfaces, in striking contrast to the opposite trend for the SrO-terminated surfaces which are characterized by $n_{xy}/n_{xz,yz} > 1$.

V. SUMMARY

The effect of Coulomb correlations on the electronic structure of $SrVO_3(001)$ surfaces was studied within the LDA+DMFT approach. The LDA single-particle electronic properties were calculated for a semi-infinite system by using the embedded Green-function approach. The layer dependent local DOS was projected on the V t_{2g} orbitals and subsequently used as an input to a DMFT calculation combined with the multiband QMC technique. The results for the SrO-layer-terminated surfaces are in qualitative agreement with previous tight-binding calculations by one of the present authors (A.L.). The reduced coordination number of outermost V atoms gives rise to a significant narrowing of the LDA DOS for the $d_{xz,yz}$ band, which leads to stronger correlation features in the quasiparticle spectra. Moreover, the surface-induced transfer of charge from $d_{xz,yz}$ to d_{xy} orbitals is enhanced due to Coulomb correlations. In the case of VO_2-layer terminated surfaces, the lack of the local octahedral symmetry at outermost V sites causes a considerable rearrangement of t_{2g} valence charge compared to the bulk, in particular, a transfer of charge from d_{xy} to $d_{xz,yz}$. This transfer is further promoted by correlation effects.

Compared to the cubic bulk environment, therefore, $SrVO_3$ surfaces exhibit a rich variety of single-particle and many-body phenomena. Apart from the simple band narrowing effect, important effects occur due to shifts of inequivalent t_{2g} bands, redistribution of spectral weight, and concomitant redistribution of orbital occupations. In addition, the issue of surface termination was studied from first principles and was shown to give rise to opposite trends with regard to orbital-dependent correlation enhancement. Analogous effects should take place also at other transition-metal oxide surfaces.

[1] M. Imada, A. Fujimori, and Y. Tokura, Rev. Mod. Phys. **70**, 1039 (1998).
[2] A. Georges, G. Kotliar, W. Krauth, and M. J. Rozenberg, Rev. Mod. Phys. **68**, 13 (1996).
[3] E. Dagotto, Rev. Mod. Phys. **66**, 763 (1994).
[4] A. Fujimori, I. Hase, H. Namatame, Y. Fujishima, Y. Tokura, H. Eisaki, S. Uchida, K. Takegahara, and F. M. F. de Groot, Phys. Rev. Lett. **69**, 1796 (1992).
[5] K. Maiti, P. Mahadevan, and D. D. Sarma, Phys. Rev. Lett. **80**, 2885 (1998).
[6] R. Matzdorf, Z. Fang, Ismail, J. Zhang, T. Kimura, Y. Tokura, K. Terakura, and E. W. Plummer, Science **289**, 746 (2000).
[7] A. Damascelli, D. H. Lu, K. M. Shen, N. P. Armitage, F. Ronning, D. L. Feng, C. Kim, Z. –X. Shen, T. Kimura, Y. Tokura, Z. Q. Mao, and Y. Maeno, Phys. Rev. Lett. **85**, 5194 (2000).
[8] K. Maiti, A. Kumar, D. D. Sarma, E. Weschke, and G. Kaindl, Phys. Rev. B **70**, 195112 (2004).
[9] K. Maiti, D. D. Sarma, M. J. Rozenberg, I. H. Inoue, H. Makino, O. Goto, M. Pedio, and R. Cimino, Europhys. Lett. **55**, 246 (2001).
[10] A. Sekiyama, H. Fujiwara, S. Imada, S. Suga, H. Eisaki, S. I. Uchida, K. Takegahara, H. Harima, Y. Saitoh, I. A. Nekrasov, G. Keller, D. E. Kondakov, A. V. Kozhenvikov, Th. Pruschke, K. Held, D. Vollhardt, and V. I. Anisimov, Phys. Rev. Lett. **93**, 156402 (2004).
[11] T. Yoshida, K. Tanaka, H. Yagi, A. Ino, H. Eisaki, A. Fujimori, and Z. X. Shen, Phys. Rev. Lett. **95**, 146404 (2005).
[12] A. Liebsch, Phys. Rev. Lett. **90**, 096401 (2003).
[13] A. Liebsch, Eur. Phys. J. B **32**, 477 (2003).
[14] D. Vollhardt, *Correlated Electron Systems*, edited by V. J. Emery (World Scientific, Singapore, 1993), p. 57.
[15] K. Held, I. A. Nekrasov, N. Blümer, V. I. Anisimov, and D. Vollhardt, Int. J. Mod. Phys. B **15**, 2611 (2001).
[16] J. E. Hirsch and R. M. Fye, Phys. Rev. Lett. **56**, 2521 (1986).
[17] R. M. Fye and J. E. Hirsch, Phys. Rev. B **38**, 433 (1988).
[18] W. Kohn and L. J. Sham, Phys. Rev. **140**, A1133 (1965).
[19] H. Ishida, Phys. Rev. B **63**, 165409 (2001).
[20] J. E. Inglesfield, J. Phys. C **14**, 3795 (1981).
[21] J. E. Inglesfield, Comput. Phys. Commun. **137**, 89 (2001).
[22] D. Wortmann, H. Ishida, and S. Blügel, Phys. Rev. B **65**, 165103 (2002).
[23] D. Wortmann, H. Ishida, and S. Blügel, Phys. Rev. B **66**, 075113 (2002).
[24] http://www.flapw.de
[25] K. Takegahara, J. Electron Spectrosc. Relat. Phenom. **66**, 303 (1995).
[26] I. A. Nekrasov, G. Keller, D. E. Kondakov, A. V. Kozhevnikov, T. Pruschke, K. Held, D. Vollhardt, and V. I. Anisimov, Phys. Rev. B **72**, 155106 (2005).
[27] I. A. Nekrasov, K. Held, G. Keller, D. E. Kondakov, T. Pruschke, M. Kollar, O. K. Andersen, V. I. Anisimov, and D. Vollhardt, cond-mat/0508313.
[28] D. Kalkstein and P. Soven, Science **26**, 85 (1971).
[29] M. Jarrel and J. E. Gubernatis, Phys. Rep. **269**, 133 (1996).